THE JOURNAL OF PHYSICAL CHEMISTRY Letters

Perspective

pubs.acs.org/JPCL

Horizontal Silicon Nanowires with Radial p−n Junctions: A Platform for Unconventional Solar Cells

Xing Zhang,[†] Christopher W. Pinion,[†] Joseph D. Christesen, Cory J. Flynn, Thomas A. Celano, and James F. Cahoon*

Department of Chemistry, University of North Carolina at Chapel Hill, Chapel Hill, North Carolina 27599-3290, United States

Supporting Information

ABSTRACT: The silicon p−n junction is the most successful solar energy technology to date, yet it accounts for a marginal percentage of worldwide energy production. To change the status quo, a disruptive technological breakthrough is needed. In this Perspective, we discuss the potential for complex silicon nanowires to serve as a platform for next-generation photovoltaic devices. We review the synthesis, electrical characteristics, and optical properties of core/shell silicon nanowires that are subwavelength in diameter and contain radial p−n junctions. We highlight the unique features of these nanowires, such as optical antenna effects that concentrate light and intense built-in electric fields that enable ultrafast charge-carrier separation. We advocate a paradigm in which nanowires are arranged in periodic horizontal arrays to form ultrathin devices. Unlike conventional planar silicon, nanowire structures provide the flexibility to incorporate multiple semiconductor, dielectric, and metallic materials in a single system, providing the foundation for a disruptive, unconventional solar energy technology.

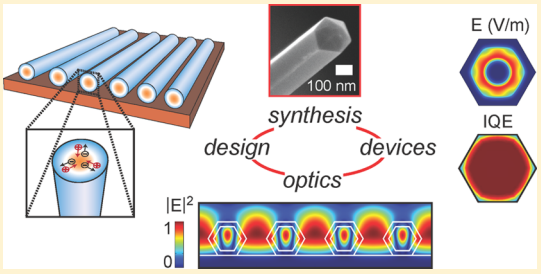

Nanostructured materials are the focus of most current efforts to design next-generation solar cells that could achieve high power conversion efficiencies at a relatively low total cost. These efforts include the development of organic bulk heterojunction devices,[1] dye-sensitized solar cells,[2] and quantum dot solar cells.[3−7] As discussed in other recent Perspectives,[1−7] the successful implementation of high-efficiency photovoltaic (PV) devices relies on careful design of the nanometer-scale morphologies and interfaces within these systems. The most unconventional devices aim to utilize third-generation solar cell concepts,[8] such as multiple exciton generation[4] (MEG) and hot carrier collection,[9] that would allow devices to exceed the Shockley−Queisser limit on power conversion efficiency.[10] For instance, a solar cell using PbSe quantum dots to enable MEG recently reported a quantum efficiency exceeding 100%.[11] Despite these promising research directions, no technology has been able to displace the reasonably good efficiency and low cost of conventional Si p−n junctions. In this Perspective, we discuss the development of complex Si nanowires (NWs) as a technology that can combine the advantages of the well-known Si p−n junction with new materials and solar energy concepts, creating a new class of unconventional PV devices.

Semiconductor NWs have become a popular platform for the development of both PV and photoelectrochemical solar energy devices.[12−15] Conventional semiconductor PV devices are formed with planar p-type/n-type (p−n) homo- or hetero-junctions, and NW devices can be formed using the same junctions by conceptually rearranging the structure into a cylindrical geometry, as illustrated in Figure 1A. The wire geometry can be formed using both bottom-up chemical synthesis,[16−18] such as vapor−liquid−solid (VLS) growth,[19] as well as top-down fabrication techniques,[20,21] such as lithographically patterned deep reactive ion etching. These radial p−n junctions have been encoded in wires with diameters ranging from nanometers to micrometers and have been realized with a variety of semiconductors, including group II−VI, III−V, and IV materials such as CdS,[22,23] GaAs[24] or GaN,[25] and Si,[16−18,21,26,27] respectively. In this Perspective, we review the current paradigms for NW-based PV devices and provide our own perspective on how bottom-up synthesis and assembly of complex NW systems based on Si can be used as a transformative new platform for the development of next-generation, high-efficiency PV structures.

> The capability to separate the direction of light propagation from the direction of charge separation is one of the most frequently discussed motivations for developing wire-based PV structures.

The capability to separate the direction of light propagation from the direction of charge separation is one of the most

Received: March 8, 2013
Accepted: May 30, 2013
Published: May 30, 2013

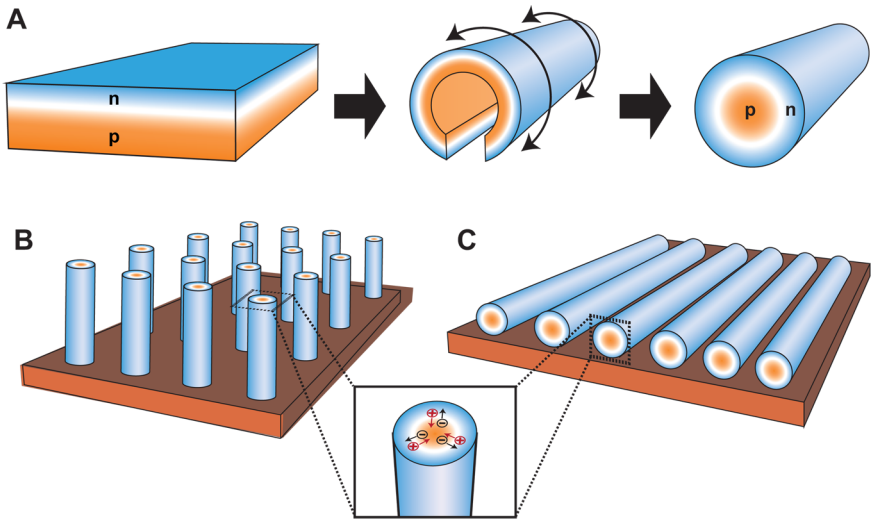

Figure 1. Overview of geometries used for semiconductor p−n junction PV devices. (A) Conventional planar p−n junction that can be conceptually rearranged into a cylindrical geometry to form a radial p−n junction NW. (B) Wire-based PV device composed of vertically oriented arrays that facilitate charge separation in the direction perpendicular to illumination. (C) NW-based PV device composed of 200−300 nm diameter NWs oriented horizontally so that the NWs are illuminated perpendicular to the wire axis and charge separation occurs in the short, radial direction.

frequently discussed motivations for developing wire-based PV structures, as illustrated in Figure 1B. In this paradigm, the NW is oriented vertically such that illumination is parallel to the wire axis and charge carriers are separated in the perpendicular, radial direction. This geometry permits high performance to be realized even with low-quality, low-cost semiconductor materials if the wire diameter equals or is less than the minority carrier diffusion length of the material.[28] In addition, vertically oriented arrays of wires have been shown to introduce antireflection, light scattering, and diffraction effects that enhance light absorption.[21,29] For Si-based PV devices, this paradigm has led to the development of micrometer diameter wire arrays that approach the efficiency of conventional planar p−n junctions.[26,27] Here, we instead focus on a paradigm, illustrated in Figure 1C, in which the NWs are oriented horizontally such that they are illuminated perpendicular to the wire axis. In this geometry, charge separation occurs in the short, radial direction, and the NWs are illuminated uniformly along their total length. We also focus on mesoscopic NWs with diameters of 200−300 nm that are well-suited to exhibit unconventional effects related to their small size. We review the synthesis, electrical characteristics, and optical properties of the Si NW structures that can be used within this paradigm to create next-generation PV structures.

The construction of NW-based thin-film PV devices can be realized through the sequential construction of increasingly complex device architectures, as depicted in Figure 2. The simplest structures (top left, Figure 2) are single-NW Si devices, which have the potential to meet high-performance metrics, as discussed below. However, to move beyond these single Si structures, two parallel technologies must be developed. First, new strategies to design, synthesize, and fabricate advanced NW heterostructures that incorporate multiple components (semiconductors, dielectrics, and metals) can be developed to utilize advanced next-generation PV concepts[8] such as hot carrier collection,[9] multiple exciton generation,[4,11] and surface-plasmon-mediated absorption enhancement.[30−33] Second, strategies to assemble, network, and integrate ensembles of individual NWs into one monolithic PV device can be developed to scale NW technology to large-area

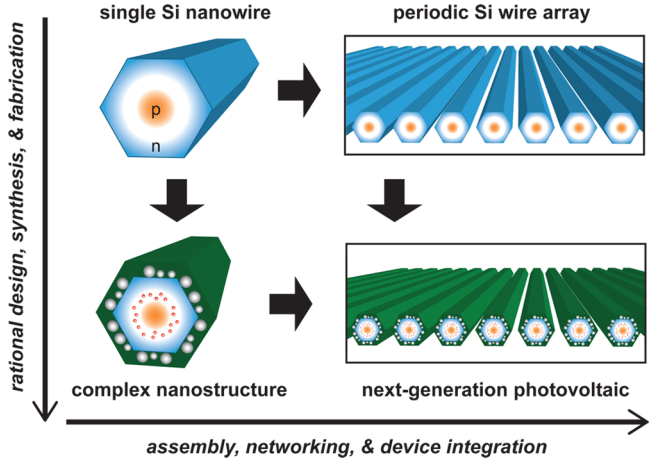

Figure 2. Overview of the general strategy for development of NW PV devices that use radial Si p−n junctions as the charge-separating scaffold for advanced solar cell architectures.

PV devices. These two directions can be pursued in parallel to develop next-generation devices based on Si NWs. Here, we primarily discuss the first challenge but note that there have been substantial advancements on the problem of NW-directed- and self-assembly.[34,35]

Recently, well-controlled methods for bottom-up synthesis of Si NWs with radial p−n junctions have been developed,[16−18,36] enabling synthesis of the high-quality core/shell PV NW structures illustrated in Figure 3. In this approach, NWs are grown by a VLS mechanism using a metal nanoparticle to catalyze growth of p-type NW cores, as shown in the SEM image in Figure 3B. Following core growth, intrinsic and n-type shells are sequentially grown by a vapor−solid (VS) mechanism to create core/shell p-type/intrinsic/n-type (p−i−n) PV structures, as shown in Figure 3C. These core/shell structures exhibit faceted surfaces with an approximately hexagonal cross section (see Figure 3D) that is indicative of a highly crystalline shell structure.[16] Details of the procedures used to synthesize NWs are provided in the Supporting Information (SI).

dx.doi.org/10.1021/jz400533v | J. Phys. Chem. Lett. 2013, 4, 2002−2009

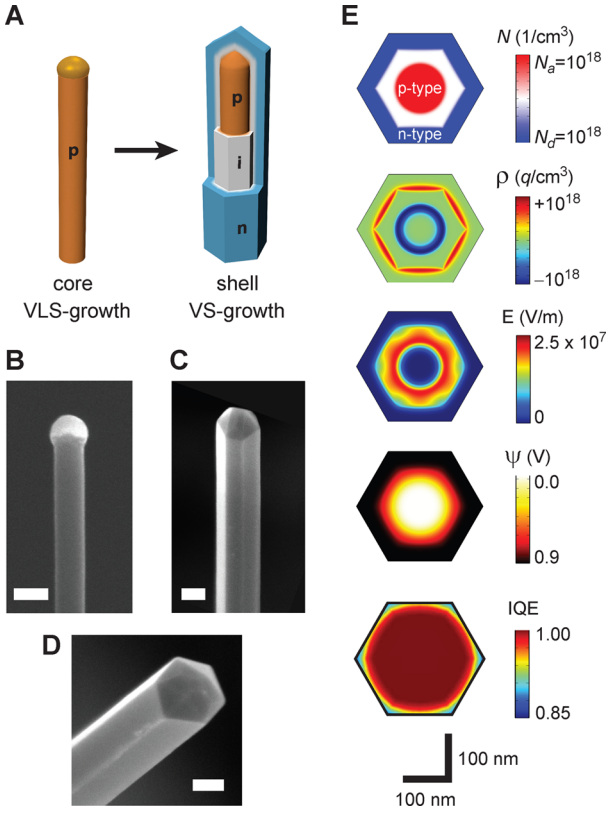

Figure 3. Synthesis and characteristics of core/shell p–i–n junction Si NWs. (A) Schematic of VLS growth of a p-type NW followed by VS growth of intrinsic and n-type shells to form p–i–n core shell/ structures. (B) SEM image of VLS-grown Si NW with a Au catalyst at the tip; scale bar, 100 nm. (C) SEM image of a core/shell p–i–n NW; scale bar, 100 nm. (D) End-on SEM image of a core/shell p–i–n NW showing a faceted, hexagonal shape with well-defined crystal planes; scale bar, 100 nm. (E) Finite-element simulations of the core/shell p–i–n junction showing, from top to bottom, the doping distribution, N, charge density distribution ρ, electric field distribution, E, electrostatic potential, ψ, and internal quantum efficiency (IQE) under optical excitation. Simulations include Auger recombination, a surface recombination velocity of 10^5 cm/s, and a minority carrier lifetime of τ_{SRH} = 10 ns.

To understand the potential PV performance of the core/shell p–i–n NW structures, we have used finite-element modeling to probe the electrical characteristics of the radial junctions. Building on our previous modeling efforts,[17] we analyzed, as illustrated in Figure 3E, the charge density, electric field, electrostatic potential, and internal quantum efficiency (IQE) values within the hexagonal cross section of the NWs. These simulation results demonstrate that with n- and p-type doping levels of 10^{18} cm^{-3} or larger, the ~250 nm diameter NW geometry yields well-defined depletion regions, intense built-in electric fields of ~10^7 V/m, and IQE values approaching unity throughout the structure. The high IQE values are a result of the short distance that minority carriers must diffuse to reach the p–n junction (<50 nm) as well as the short width (~40 nm) and high electric field strength within the intrinsic region. Interestingly, these short length scales and strong electric fields are sufficient to induce charge-carrier separation on ultrafast time scales of a picosecond or less (see Figure S1, SI). The combination of short length and time scales suggests that these NWs could be interesting structures to exploit unconventional third-generation PV concepts,[8] as discussed below.

To experimentally evaluate the performance of the NWs, PV devices composed of single NWs have been fabricated following literature procedures.[16,17] An SEM image of a final device is depicted in Figure 4A, which shows Ohmic metal contacts selectively defined to the p-type NW core and the n-type NW shell. As illustrated by the black curve in Figure 4B, experimental current density–voltage (J–V) measurements on these single-NW devices under simulated 1 sun AM1.5G illumination yield J–V curves that are well fit to the ideal diode equation[37] and possess an open-circuit voltage (V_{OC}) of 0.485 V, fill factor (FF) of 0.70, and short-circuit current density (J_{SC}) of 6.5 mA/cm^2. Note that J_{SC} values of up to ~10 mA/cm^2 have been reported for single-NW devices[16,17] if they are coated with conformal dielectric shells,[38] as discussed below.

An alloyed nanowire structure represents a promising route to create a single-junction photovoltaic device that is not limited by the absorption characteristics of one material.

To analyze the measured performance metrics, we have directly compared the experimental J–V curve to simulated J–V curves (red dashed lines in Figure 3B) that include values for the Shockley–Read–Hall (SRH) minority carrier lifetime, τ_{SRH}, ranging from 1 ns to 1 μs.[17] The accuracy of the device simulations has been verified by the excellent agreement with experimental J–V curves[17] as well as by independent measurement of device metrics using ultrafast microscopy.[39] The simulated J–V curves indicate that the performance of the measured device is limited not by surface or Auger recombination processes but instead by a SRH minority carrier lifetime of τ_{SRH} = 10 ns.[17] While current device parameters fall short of bulk Si PV devices, if the minority carrier lifetime in the radial NWs can be improved by 2 orders of magnitude to 1 μs, then the V_{OC} could be increased to values greater than 0.60 V. This value is comparable to those achieved in standard bulk Si solar cell modules. Recent experimental measurements have determined that minority carrier lifetimes exceeding 500 ns can be achieved in VLS-grown Si wires,[26] and experiments are in progress to achieve these values in radial p–i–n NWs.

To improve the 1 sun power conversion efficiency (η) of NW solar cells, it is also necessary to increase the J_{SC} of the devices by enhancing light absorption within the structures. In Figure 4C, we project the η of NW devices for J_{SC} values ranging from 1 to 40 mA/cm^2. This projection demonstrates that with a J_{SC} of ~40 mA/cm^2, Si NW structures could achieve an η of ~16.7% with the current τ_{SRH} of 10 ns and an η of ~21.8% with an improved τ_{SRH} of 1 μs. Note that the upper limit on J_{SC} and η for Si under 1 sun illumination is ~42 mA/cm^2 and ~31%,[10] respectively; however, charge-carrier generation that utilizes unconventional third-generation PV concepts could potentially yield higher values, as discussed below.

To achieve enhanced light absorption in NW devices, the absorption characteristics of the structures can be controlled through careful modulation of shape and composition. Because the NWs are subwavelength in diameter, they behave as cavities

dx.doi.org/10.1021/jz400533v | J. Phys. Chem. Lett. 2013, 4, 2002–2009

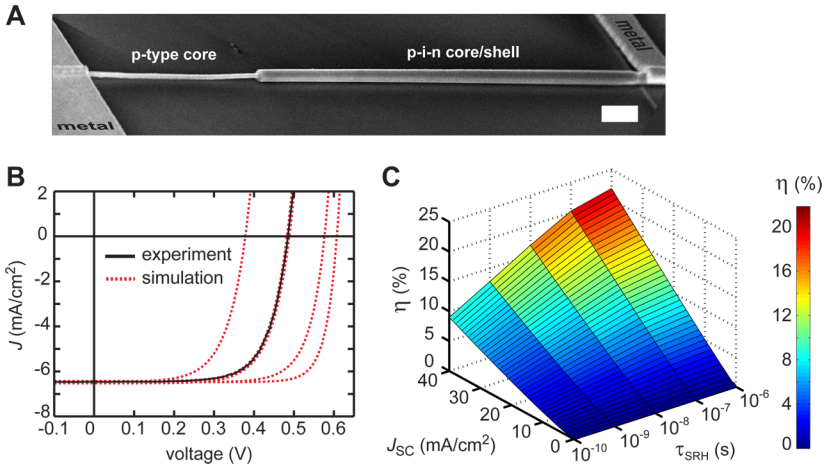

Figure 4. Performance of single core/shell p−i−n Si NW photovoltaic devices. (A) SEM image of a device showing selective metal contacts to the p-type core and n-type shell; scale bar, 1 μm. (B) Experimental (black) and simulated (dashed red) $J-V$ curves for NW devices under simulated 1 sun illumination. Simulation curves reflect, from left to right, minority carrier lifetimes of τ_{SRH} = 1, 10, 100, and 1000 ns, respectively, and all simulations include a surface recombination velocity of 100 cm/s. (C) Projected 1 sun power conversion efficiency, η, for NW devices with values of J_{SC} ranging from 0 to 40 mA/cm^2 and τ_{SRH} ranging from 100 ps to 1 μs, including a surface recombination velocity of 100 cm/s.

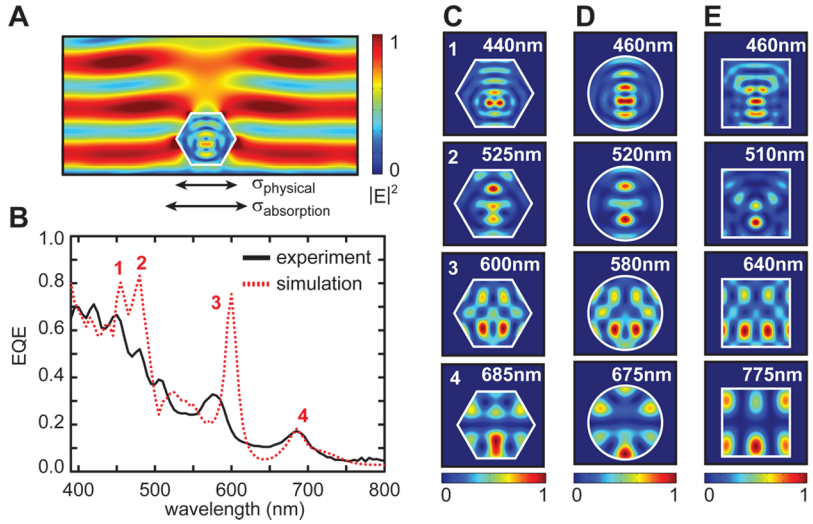

Figure 5. Optical absorption characteristics of individual Si NWs. (A) Normalized electric field ($|E|^2$) profile for an electromagnetic plane wave with a wavelength of 450 nm that is vertically incident on a single NW in which the absorption cross section ($\sigma_{absorption}$) exceeds the physical cross section ($\sigma_{physical}$). (B) Experimental (solid black) and simulated (dashed red) EQE spectra for a single Si NW with a diameter of 310 nm. (C) Resonant absorption mode profiles for the four peaks labeled 1−4 in panel B and a NW with a hexagonal cross section. (D) Absorption mode profiles for a NW with a circular cross section. (E) Absorption mode profiles for a NW with a square cross section. For panels C−E, NW diameters (lateral widths) are 310 nm, the light polarization is transverse-electric (TE) for modes 1 and 3 and transverse-magnetic (TM) for modes 2 and 4, and the wavelength for each resonant mode is denoted in the top right-hand corner of each image.

that give rise to strong optical resonances,[36,40] as illustrated by the finite-difference frequency domain optical simulations in Figure 5. In these simulations, 1 sun illumination is simulated with a vertically incident plane wave, which strongly interacts with the NWs at specific wavelengths, as exemplified in Figure 5A. As reported previously,[16] these absorption modes can result in external quantum efficiency (EQE) values that exceed unity at specific diameters and wavelengths. This phenomena, termed an optical antennae effect, results from an absorption cross section that exceeds the physical cross section of the NW and is a unique feature of the subwavelength NW structures.[16,36,41] These resonances can be experimentally quantified by direct measurement of the EQE spectra of single-NW devices, as shown by the black curve in Figure 5B (see the SI for experimental details). The experimental EQE spectrum is in good agreement with optical simulations of the absorption efficiency, shown as the dashed red curve in Figure 5B. The spectra show four prominent high-amplitude peaks, labeled 1−4, and the spatial absorption mode profiles for these peaks are illustrated in Figure 5C. These profiles consist of complex modes that have attributes of both whispering gallery and Fabry−Perot optical resonances.[36] The spectral position and amplitude of these optical absorption resonances can be tuned throughout the visible wavelengths by subtle changes in the size and shape of the NW structure.[36] The alterations in shape (hexagonal, circular, or square) modify the wavelength and appearance of the absorption modes, as illustrated by a comparison of the modes in Figure 4C−E (also see Figure S2 (SI) for full spectra for each geometry).

dx.doi.org/10.1021/jz400533v | J. Phys. Chem. Lett. 2013, 4, 2002−2009

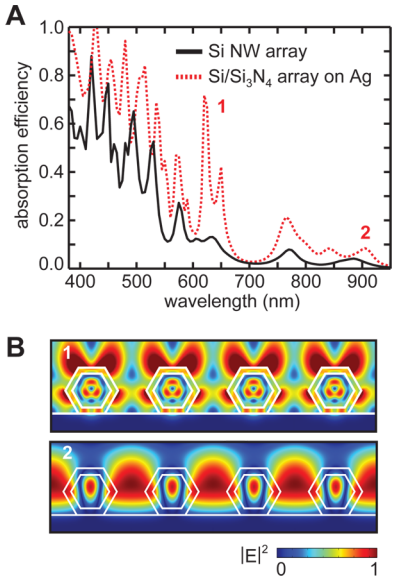

Figure 6. Optical absorption characteristics of extended arrays of Si NWs. (A) Absorption efficiency spectra of NWs on substrates composed of Si_3N_4 (black curve) and Ag (dashed red curve). Simulations reflect an infinite array of 250 nm diameter Si NWs with a gap of 200 nm between each wire. (B) Normalized electric field ($|E|^2$) profiles for the absorption resonances labeled 1 and 2 in panel A.

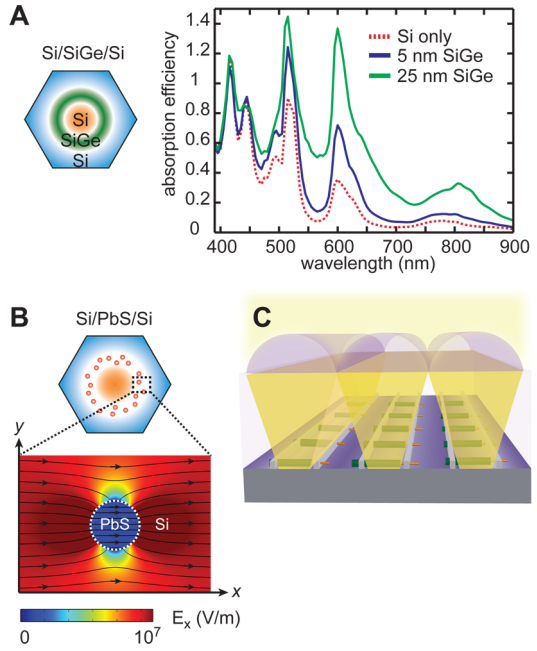

Figure 7. Concepts for PV devices using more complex nanostructures based on a Si NW platform. (A) Left, schematic of a core/shell Si NW in which the shell has been alloyed with Ge. Right, absorption efficiency spectra for NWs with no Ge (dashed red) as well as 5 (blue) and 25 nm (green) of $Si_{0.5}Ge_{0.5}$ alloy incorporated in the intrinsic region of the NW shell. (B) Top, schematic of a core/shell Si NW in which PbS quantum dots have been embedded within the intrinsic region of the core/shell p−i−n Si NW structure. Bottom, plot of the electric field lines surrounding a quantum dot embedded in a Si NW. (C) Schematic (not to scale) of a large-area microconcentrator NW array PV device, which utilizes a lenticular lens array to focus incoming 1 sun radiation onto periodic horizontal arrays of NWs.

To produce thin-film PV devices, the NWs can be arranged in periodic horizontal arrays, as indicated in Figure 2. As an instructive example, we consider here the simulated absorption efficiency of an array of 250 nm diameter Si NWs arranged with a pitch of 450 nm and a total areal filling fraction of ∼55%, as shown in Figure 6A. Despite the low filling fraction, the J_{SC} for this array, 6.26 mA/cm^2, is ∼82% of the value for a single-NW device and ∼77% of the value for a close-packed array. To increase light absorption, individual NWs can be coated with dielectric shells[38] such as 50 nm thick Si_3N_4, and the array can be placed on a reflective substrate such as Ag. The addition of these two optical effects increases the J_{SC} value by ∼72% to 10.78 mA/cm^2. As evident from a comparison of the absorption efficiency plots in Figure 6A, the improved J_{SC} value is a result of both an increase in amplitude of nearly all absorption modes as well as the appearance of prominent absorption modes at longer wavelengths. The electric field profiles for two of these long-wavelength modes are illustrated in Figure 6B, and these modes result from resonance effects from the reflective Ag substrate. Further design of complex reflective substrates and metallic nanostructures that support plasmon resonances[30−33] could be a promising direction to further boost light absorption within these NW structures using optical effects.

Despite the promising optical properties of Si NWs, the extent of light absorption in these PV structures will eventually be limited by the absorption coefficient of the material. This issue is a substantial limitation for Si because it is an indirect band gap semiconductor. As a result, the typical thickness of a planar bulk Si solar cell is 100 μm or more in order to achieve complete absorption from the ultraviolet through near-infrared wavelengths. To overcome the limitations imposed by a single material, the Si NW structures can be blended with other semiconductors to form complex heterostructure or alloy materials. For instance, the Si shell can be alloyed with Ge to create Si_xGe_{1-x} structures in which the band gap is continuously tunable between the value for Si, 1.12 eV, and that for Ge, 0.66 eV. Si_xGe_{1-x} alloys have been successfully used in multijunction amorphous Si solar cell devices,[42] and the synthesis of crystalline Ge shells on Si NWs has been reported.[43,44] As illustrated in Figure 7A, we consider here the incorporation of a 5−25 nm layer of a crystalline $Si_{0.5}Ge_{0.5}$ alloy within the intrinsic region of the NW devices to create a Si/SiGe/Si core/shell/shell structure. Although the experimental implementation of this structure would require careful consideration of band alignments and band bending at the heterojunction, we assume for the purposes of this discussion that the devices would have an IQE of unity. As indicated by the absorption efficiency spectra in Figure 7A, the presence of this thin layer substantially enhances the absorption efficiency for wavelengths greater than ∼500 nm. The incorporation of a 25 nm thick $Si_{0.5}Ge_{0.5}$ shell increases the J_{SC} of a single NW by 235% to a value of 18.0 mA/cm^2. If incorporated in the horizontal NW array discussed above (Figure 6), the Si/SiGe/Si NW would produce a J_{SC} value of 20.7 mA/cm^2. Thus, an alloyed NW structure represents a promising route to create a single-junction Si PV device that is not limited by the absorption characteristics of one material.

There has also been widespread interest in the development of unconventional solar cell devices that could achieve high efficiencies by exploiting third-generation solar cell concepts such as hot carrier collection and MEG.[8] In particular, research efforts have focused on the potential of semiconductor quantum dots (QDs) to facilitate efficient MEG processes.[4,11] In the context of Si NWs, we suggest that QD materials such as

dx.doi.org/10.1021/jz400533v | J. Phys. Chem. Lett. 2013, 4, 2002−2009

PbS or PbSe could be embedded within the Si shell, as illustrated in Figure 7B. QDs could be deposited on Si NWs by physical vapor deposition processes or, as recently reported, atomic layer deposition.[45] Experimental implementation of this structure would require careful consideration of the Si/chalcogenide interface to avoid recombination centers and diffusion of chalcogenide material into the Si NW. Depositing QD structures affords the two-fold advantage of introducing a direct band gap semiconductor absorber as well as a material that could enable MEG effects. If embedded within the intrinsic region of core/shell p−i−n NWs, the strong built-in electric field of ~10^7 V/m, as illustrated in Figure 7B, could be used to rapidly and efficiently separate hot charge carriers within QDs on a subpicosecond time scale.

If embedded within the intrinsic region of core/shell p−i−n NWs, the strong built-in electric field of ~10^7 V/m could be used to rapidly and efficiently separate hot charge carriers within QDs on a subpicosecond time scale.

If high-efficiency devices based on Si NWs with radial p−n junctions are developed, these materials might be most effectively used in a microconcentrator solar cell design,[46] which would focus light onto a series of horizontal Si NW arrays. This design uses a lenticular lens composed of an array of cylindrical lenses to concentrate 1 sun illumination, as illustrated in Figure 7C. For mild solar concentration, this design would represent an approximately 10-fold reduction in the amount of NW material needed to cover a macroscopic area. This design would also permit the fabrication of metal contacts to the NW p-type core and n-type shell that do not shadow the active, illuminated device region.

In this Perspective, we have presented a new paradigm for NW-based solar energy devices that uses horizontal arrays of high-efficiency Si NW structures. In addition, we have summarized the synthetic methods to create these structures, analyzed the current and hypothetical performance of NW devices, evaluated the unique optical characteristics of the structures, and speculated about potential future structures that could exploit the novel features of NW systems. Substantial progress on the development of NW PV devices has been made over the last several years, and substantial work still remains to realize the full potential of these systems. The combination of material flexibility and unique optical characteristics makes Si NWs an exciting platform for the development of unconventional solar energy devices.

■ ASSOCIATED CONTENT

Supporting Information

Description of the finite-element modeling, summary of experimental methods, and Figures S1−S3, showing the time scale of charge carrier separation in radial p−i−n devices, simulated absorption efficiency spectra of single NWs with different cross-sectional shapes, and polarization-resolved external quantum efficiency spectra. This material is available free of charge via the Internet at http://pubs.acs.org.

■ AUTHOR INFORMATION

Corresponding Author

*E-mail: jfcahoon@unc.edu.

Author Contributions

†X.Z. and C.W.P. contributed equally.

Notes

The authors declare no competing financial interest.

Biographies

Xing Zhang received his B.S. in Materials Science and Engineering from Tsinghua University, Beijing, China. Currently, he is a Ph.D. student in the Curriculum in Applied Science and Engineering at UNC-Chapel Hill under the direction of James Cahoon. His research interests are focused on silicon nanowire synthesis with an emphasis on developing third-generation photovoltaic devices.

Christopher W. Pinion received a B.S. in Chemistry and Physics from the University of South Carolina in 2012. He is currently pursuing his Ph.D. in Chemistry at UNC-Chapel Hill under the guidance of James Cahoon, with whom he examines the precise control of axial nanowire heterostructures for optoelectronics.

Joseph D. Christesen received a B.S. in Chemistry and Computer Science from The College of William and Mary in 2011. He is currently a Ph.D. candidate in Chemistry at UNC-Chapel Hill, where he synthesizes shape-controlled nanowire structures for use in photonic and plasmonic devices in James Cahoon's group.

Cory J. Flynn graduated from Wright State University in 2011 with a B.S. in Chemistry. He is currently a Ph.D. candidate in Chemistry at UNC-Chapel Hill under the guidance of James Cahoon, where his research focuses on controlling the morphology and material quality of p-type metal oxide semiconductors.

Thomas A. Celano graduated from North Carolina State University in 2011 with a B.S. in Chemistry. He is currently a Ph.D. student in Chemistry at UNC-Chapel Hill in the Cahoon group. His research focuses on assembly of silicon nanowire arrays for use in photovoltaic devices.

James F. Cahoon received his B.S. in Chemistry and Philosophy from The College of William and Mary in 2003 and his Ph.D. in Physical Chemistry from UC-Berkeley in 2008, where he worked in the field of ultrafast vibrational spectroscopy with Charles Harris. Beginning in 2009, he worked as an I.C. postdoctoral fellow with Charles Lieber at Harvard University, and he began his independent career at UNC-Chapel Hill in 2011. His group combines synthetic control of semiconductor nanomaterials with detailed physical characterization and modeling to rationally design new functional materials. Webpage: www.chem.unc.edu/people/faculty/cahoon.

■ ACKNOWLEDGMENTS

We acknowledge support of this research from start-up funding from UNC-Chapel Hill.

■ REFERENCES

(1) He, F.; Yu, L. P. How Far Can Polymer Solar Cells Go? In Need of a Synergistic Approach. *J. Phys. Chem. Lett.* **2011**, *2*, 3102−3113.
(2) Peter, L. M. The Gratzel Cell: Where Next? *J. Phys. Chem. Lett.* **2011**, *2*, 1861−1867.
(3) Kamat, P. V. Quantum Dot Solar Cells. The Next Big Thing in Photovoltaics. *J. Phys. Chem. Lett.* **2013**, 908−918.
(4) Beard, M. C. Multiple Exciton Generation in Semiconductor Quantum Dots. *J. Phys. Chem. Lett.* **2011**, *2*, 1282−1288.
(5) Toyoda, T.; Shen, Q. Quantum-Dot-Sensitized Solar Cells: Effect of Nanostructured TiO_2 Morphologies on Photovoltaic Properties. *J. Phys. Chem. Lett.* **2012**, *3*, 1885−1893.

(6) Mora-Seró, I.; Bisquert, J. Breakthroughs in the Development of Semiconductor-Sensitized Solar Cells. *J. Phys. Chem. Lett.* **2010**, *1*, 3046−3052.
(7) Hetsch, F.; Xu, X.; Wang, H.; Kershaw, S. V.; Rogach, A. L. Semiconductor Nanocrystal Quantum Dots as Solar Cell Components and Photosensitizers: Material, Charge Transfer, and Separation Aspects of Some Device Topologies. *J. Phys. Chem. Lett.* **2011**, *2*, 1879−1887.
(8) Green, M., A. *Third Generation Photovoltaics: Advanced Solar Energy Conversion*; Springer: Heidelberg, Germany, 2003.
(9) Tisdale, W. A.; Williams, K. J.; Timp, B. A.; Norris, D. J.; Aydil, E. S.; Zhu, X. Y. Hot-Electron Transfer from Semiconductor Nanocrystals. *Science* **2010**, *328*, 1543−1547.
(10) Shockley, W.; Queisser, H. J. Detailed Balance Limit of Efficiency of p−n Junction Solar Cells. *J. Appl. Phys.* **1961**, *32*, 510−519.
(11) Semonin, O. E.; Luther, J. M.; Choi, S.; Chen, H. Y.; Gao, J. B.; Nozik, A. J.; Beard, M. C. Peak External Photocurrent Quantum Efficiency Exceeding 100% via MEG in a Quantum Dot Solar Cell. *Science* **2011**, *334*, 1530−1533.
(12) Kempa, T. J.; Day, R. W.; Kim, S.-K.; Park, H.-G.; Lieber, C. M. Semiconductor Nanowires: A Platform for Exploring Limits and Concepts for Nano-Enabled Solar Cells. *Energy Environ. Sci.* **2013**, *6*, 719−733.
(13) Garnett, E. C.; Brongersma, M. L.; Cui, Y.; McGehee, M. D. Nanowire Solar Cells. In *Annual Review of Materials Research*; Clarke, D. R., Fratzl, P., Eds.; Annual Reviews: Palo Alto, CA, 2011; Vol. *41*, pp 269−295.
(14) Hochbaum, A. I.; Yang, P. D. Semiconductor Nanowires for Energy Conversion. *Chem. Rev.* **2010**, *110*, 527−546.
(15) Peng, K. Q.; Lee, S. T. Silicon Nanowires for Photovoltaic Solar Energy Conversion. *Adv. Mater.* **2011**, *23*, 198−215.
(16) Kempa, T. J.; Cahoon, J. F.; Kim, S.-K.; Day, R. W.; Bell, D. C.; Park, H.-G.; Lieber, C. M. Coaxial Multishell Nanowires with High-Quality Electronic Interfaces and Tunable Optical Cavities for Ultrathin Photovoltaics. *Proc. Natl. Acad. Sci. U.S.A.* **2012**, *109*, 1407−1412.
(17) Christesen, J. D.; Zhang, X.; Pinion, C. W.; Celano, T. A.; Flynn, C. J.; Cahoon, J. F. Design Principles for Photovoltaic Devices Based on Si Nanowires with Axial or Radial p−n Junctions. *Nano Lett.* **2012**, *12*, 6024−6029.
(18) Tian, B. Z.; Zheng, X. L.; Kempa, T. J.; Fang, Y.; Yu, N. F.; Yu, G. H.; Huang, J. L.; Lieber, C. M. Coaxial Silicon Nanowires as Solar Cells and Nanoelectronic Power Sources. *Nature* **2007**, *449*, 885−889.
(19) Schmidt, V.; Wittemann, J. V.; Gosele, U. Growth, Thermodynamics, and Electrical Properties of Silicon Nanowires. *Chem. Rev.* **2010**, *110*, 361−388.
(20) Peng, K. Q.; Xu, Y.; Wu, Y.; Yan, Y. J.; Lee, S. T.; Zhu, J. Aligned Single-Crystalline Si Nanowire Arrays for Photovoltaic Applications. *Small* **2005**, *1*, 1062−1067.
(21) Garnett, E.; Yang, P. D. Light Trapping in Silicon Nanowire Solar Cells. *Nano Lett.* **2010**, *10*, 1082−1087.
(22) Fan, Z. Y.; Razavi, H.; Do, J. W.; Moriwaki, A.; Ergen, O.; Chueh, Y. L.; Leu, P. W.; Ho, J. C.; Takahashi, T.; Reichertz, L. A.; et al. Three-Dimensional Nanopillar-Array Photovoltaics on Low-Cost and Flexible Substrates. *Nat. Mater.* **2009**, *8*, 648−653.
(23) Tang, J.; Huo, Z.; Brittman, S.; Gao, H.; Yang, P. Solution-Processed Core−Shell Nanowires for Efficient Photovoltaic Cells. *Nat. Nanotechnol.* **2011**, *6*, 568−572.
(24) Colombo, C.; Heibeta, M.; Gratzel, M.; Fontcuberta i Morral, A. Gallium Arsenide p−i−n Radial Structures for Photovoltaic Applications. *Appl. Phys. Lett.* **2009**, *94*, 173108.
(25) Dong, Y.; Tian, B.; Kempa, T. J.; Lieber, C. M. Coaxial Group III−Nitride Nanowire Photovoltaics. *Nano Lett.* **2009**, *9*, 2183−2187.
(26) Kelzenberg, M. D.; Turner-Evans, D. B.; Putnam, M. C.; Boettcher, S. W.; Briggs, R. M.; Baek, J. Y.; Lewis, N. S.; Atwater, H. A. High-Performance Si Microwire Photovoltaics. *Energy Environ. Sci.* **2011**, *4*, 866−871.
(27) Putnam, M. C.; Boettcher, S. W.; Kelzenberg, M. D.; Turner-Evans, D. B.; Spurgeon, J. M.; Warren, E. L.; Briggs, R. M.; Lewis, N. S.; Atwater, H. A. Si Microwire-Array Solar Cells. *Energy Environ. Sci.* **2010**, *3*, 1037−1041.
(28) Kayes, B. M.; Atwater, H. A.; Lewis, N. S. Comparison of the Device Physics Principles of Planar and Radial p−n Junction Nanorod Solar Cells. *J. Appl. Phys.* **2005**, *97*, 114302−114311.
(29) Kelzenberg, M. D.; Boettcher, S. W.; Petykiewicz, J. A.; Turner-Evans, D. B.; Putnam, M. C.; Warren, E. L.; Spurgeon, J. M.; Briggs, R. M.; Lewis, N. S.; Atwater, H. A. Enhanced Absorption and Carrier Collection in Si Wire Arrays for Photovoltaic Applications. *Nat. Mater.* **2010**, *9*, 239−244.
(30) Ferry, V. E.; Munday, J. N.; Atwater, H. A. Design Considerations for Plasmonic Photovoltaics. *Adv. Mater.* **2010**, *22*, 4794−4808.
(31) Hägglund, C.; Apell, S. P. Plasmonic Near-Field Absorbers for Ultrathin Solar Cells. *J. Phys. Chem. Lett.* **2012**, *3*, 1275−1285.
(32) Atwater, H. A.; Polman, A. Plasmonics for Improved Photovoltaic Devices. *Nat. Mater.* **2010**, *9*, 205−213.
(33) Cho, C. H.; Aspetti, C. O.; Turk, M. E.; Kikkawa, J. M.; Nam, S. W.; Agarwal, R. Tailoring Hot-Exciton Emission and Lifetimes in Semiconducting Nanowires via Whispering-Gallery Nanocavity Plasmons. *Nat. Mater.* **2011**, *10*, 669−675.
(34) Long, Y. Z.; Yu, M.; Sun, B.; Gu, C. Z.; Fan, Z. Y. Recent Advances in Large-Scale Assembly of Semiconducting Inorganic Nanowires and Nanofibers for Electronics, Sensors and Photovoltaics. *Chem. Soc. Rev.* **2012**, *41*, 4560−4580.
(35) Wang, M. C. P.; Gates, B. D. Directed Assembly of Nanowires. *Mater. Today.* **2009**, *12*, 34−43.
(36) Kim, S.-K.; Day, R. W.; Cahoon, J. F.; Kempa, T. J.; Song, K.-D.; Park, H.-G.; Lieber, C. M. Tuning Light Absorption in Core/Shell Silicon Nanowire Photovoltaic Devices through Morphological Design. *Nano Lett.* **2012**, *12*, 4971−4976.
(37) Gray, J. L. The Physics of the Solar Cell. In *Handbook of Photovoltaic Science and Engineering*; Antonio Luque, S. H., Ed.; John Wiley and Sons: Chichester, U.K., 2004; pp 61−112.
(38) Yu, Y.; Ferry, V. E.; Alivisatos, A. P.; Cao, L. Dielectric Core−Shell Optical Antennas for Strong Solar Absorption Enhancement. *Nano Lett.* **2012**, *12*, 3674−3681.
(39) Gabriel, M. M.; Kirschbrown, J. R.; Christesen, J. D.; Pinion, C. W.; Zigler, D. F.; Grumstrup, E. M.; Mehl, B. P.; Cating, E. E. M.; Cahoon, J. F.; Papanikolas, J. M. Direct Imaging of Free Carrier and Trap Carrier Motion in Silicon Nanowires by Spatially-Separated Femtosecond Pump−Probe Microscopy. *Nano Lett.* **2013**, *13*, 1336−1340.
(40) Cao, L.; White, J. S.; Park, J.-S.; Schuller, J. A.; Clemens, B. M.; Brongersma, M. L. Engineering Light Absorption in Semiconductor Nanowire Devices. *Nat. Mater.* **2009**, *8*, 643−647.
(41) Cao, L. Y.; Fan, P. Y.; Vasudev, A. P.; White, J. S.; Yu, Z. F.; Cai, W. S.; Schuller, J. A.; Fan, S. H.; Brongersma, M. L. Semiconductor Nanowire Optical Antenna Solar Absorbers. *Nano Lett.* **2010**, *10*, 439−445.
(42) Reece, S. Y.; Hamel, J. A.; Sung, K.; Jarvi, T. D.; Esswein, A. J.; Pijpers, J. J. H.; Nocera, D. G. Wireless Solar Water Splitting Using Silicon-Based Semiconductors and Earth-Abundant Catalysts. *Science* **2011**, *334*, 645−648.
(43) Ben-Ishai, M.; Patolsky, F. A Route to High-Quality Crystalline Coaxial Core/Multishell Ge@Si$(GeSi)_n$ and Si@$(GeSi)_n$ Nanowire Heterostructures. *Adv. Mater.* **2010**, *22*, 902−906.
(44) Lauhon, L. J.; Gudiksen, M. S.; Wang, C. L.; Lieber, C. M. Epitaxial Core−Shell and Core−Multishell Nanowire Heterostructures. *Nature* **2002**, *420*, 57−61.
(45) Dasgupta, N. P.; Jung, H. J.; Trejo, O.; McDowell, M. T.; Hryciw, A.; Brongersma, M.; Sinclair, R.; Prinz, F. B. Atomic Layer Deposition of Lead Sulfide Quantum Dots on Nanowire Surfaces. *Nano Lett.* **2011**, *11*, 934−940.
(46) Yoon, J.; Baca, A. J.; Park, S. I.; Elvikis, P.; Geddes, J. B.; Li, L. F.; Kim, R. H.; Xiao, J. L.; Wang, S. D.; Kim, T. H.; et al. Ultrathin Silicon Solar Microcells for Semitransparent, Mechanically Flexible

and Microconcentrator Module Designs. *Nat. Mater.* **2008**, *7*, 907−915.